International Journal of Science and Research (IJSR)
ISSN (Online): 2319-7064
Index Copernicus Value (2016): 79.57 | Impact Factor (2015): 6.391

Effects of MHD on Peristalsis Transport and Heat Transfer with Variables Viscosity in Porous Medium

Mohammed R. Salman[1], Ahmed M. Abdulhadi[2]

University of Baghdad-College of Science-Department of Math-Baghdad-Iraq

Abstract: ***The paper is a study on the peristaltic transport of a magnetohydro dynamic fluid in an asymmetric tapered channel with porous medium. The study is the prominent motivated for the phenomenon of peristalsis in the flow of some physiological fluids in the human body devices. The viscosity of the fluid is dependent on temperature. The basic problems associated with heat and mass transfer during the fluids flow. The study has been carried out for long wavelength of the peristaltic motion. By using perturbation technique, series solutions have been obtained for stream function, velocity, pressure gradient, shear stress and pressure rise per wavelength with low Reynolds number. It is seen that the results of the study reveals that the pressure gradient is decrease with increasing of Hartmann number and the thermal radiation parameter and mean flow rate, but increases with increasing the slip velocity. The average rise in pressure increases with the increase of Grashof number while it decreases by increasing of Hartmann number. The velocity is increasing with increase of Hartmann number and the thermal radiation parameter at the core part of the channel. The study reveals also that the volume of the trapping bolus increases with increases of Reynolds model viscosity, while decreasing with increase of Hartmann number. In order to illustrate the validity of the theoretical study, numerical results have been computed by using MATHEMATICA software.***

Keywords: Peristaltic transport, Reynolds number, Hartmann number, MHD Fluid, Porous Medium

1. Introduction

The peristaltic transport is a unique mechanism for pumping most various physiological fluids, such as blood flow in small veins and arteries of the blood circulation in the human body, transferring the ovum in the Fallopian tube and the movement of sperm in the channels, transfer the yellow substance from the gallbladder to the twelve, transfer of urine from the kidney to the bladder through the ureter, the transfer of nutrients in the gastrointestinal tract, is performed with the aid of peristaltic mechanism and there are important applications in many biomedical devices, such as blood pumps and heart lung machines. The physiology of the gastrointestinal tract, esophagus, stomach, intestine and ureter associated with the phenomenon of peristalsis was discussed in the book "Biomathematics" [13]. There are several important research studies on the peristalsisly transmission of fluids,, among them, Usha [30] and Fung [31] and Shapiro et al.[4] and Mekheimer [19] and There are also some recent Important studies in noxious transient fluids on peristaltic transport include those by Misra and Maiti [14–16], [23-25] also Misra and Pandey[17, 18] and Hayat and Ali.[21] and Tripathy [9] and Afifi [1] and Eytan et al.[10].

Peristaltic flow of a multi-layered power-law fluid in a cylindrical vessel was studied by Misra and Pandey [17]. The same authors [18] also performed analysis of peristaltic flow of a Casson fluid in both two-dimensional and 3-dimensional cases, by considering the existence of a peripheral layer of Newtonian fluid. On the other study, Misra and Maiti [15] made an important observation that the nature of trajectories of fluid particles during peristaltic flow plays a significant role in the proper functioning in arterioles of the micro-circulatory system. they further observed that the characteristics of peristaltic transport of the fluid along with velocity distribution and shear stress distribution at the wall are significantly affected by the amplitude ratio of the waves. It is to be noted that in the aforesaid studies of peristaltic flow of various types of fluids under different situations, the associated problems of heat and mass transfer. Neither do they take into account the temperature dependence of the fluid properties. As we know, heat transfer fundamentally refers to the exchange of thermal energy between the diffe-rent components of a physical system.

Presented Pfeffer and Happel [22], examined an analytical solution to a problem of estimating particle to-fluid heat and mass transfer rates in multiparticle systems at low Reynolds numbers. A problem of heat and mass transfer during MHD flow of a viscous fluid in a vertical plate was discussed by Singh et al.[8], by considering the fluid to be incompressible and electrically conducting. The vertical plate was assumed to be porous and to be embedded in a porous medium.

There have been studies in recent years to the effects of heat and mass transfer on MHD channel flows were investigated recently by Gul et al.[2, 3] the authors made an important observation that for both ferrofluids and nano-fluids, the fluid velocity and temperature are highly influenced by fluid viscosity and thermal conductivity. It was remarked on the basis of the study [3] that in comparison with water, ethylene glycol is considered as a better base fluid for convection owing to the fact that its viscosity and thermal conductivity are higher than those of water. Zin et al.[20] and Khalid et al.[5] deal with two different problems of MHD free convection flows past vertical plates embedded in porous media. In [20], the fluid considered is a Jeffrey fluid containing nano-particles of silver. They observed that a rise in volume fraction is accompanied by an increase in fluid velocity and a rise in fluid temperature.

As well a study presented by Mishra et al.[26], the effect of heat and mass transfer on free convective flow of an incompressible viscoelastic fluid, by considering the fluctuative suction to be time-dependent and he presented Sinha and Misra [7] studied the effect of induced magnetic field on MHD stagnation point flow on a stretching heat, by accounting for the heat transfer. In a recent communication, and by Misra and Adhikary [12] presented their study on MHD oscillatory channel flow, heat and mass transfer in the presence of a chemical reaction. On the basis of this study, the authors reported that heat transfer increases with increasing Prandtl number and also that the mass transfer rate enhances with a reduction in the value of Schmidt number (mass diffusivity).

In a study on the neutron fluid carried out, Srinivas and Gayathri [27] examined the influence of heat transfer on the peristaltic flow in a vertical channel flow asymmetry was supposed to be due to propagation of wave train of different amplitude and porous medium. Hayat et al.[29] studied the influence of velocity-slip and thermal slip on peristaltic flow in an asymmetric channel, in this study the effects of heat and mass transfer, and the temperature-dependence of the fluid properties on peristaltic flow. A recent studies have also been iscussed, Misra et al.[11] the influence of heat and mass transfer in asymmetric channels during peristaltic transport of an MHD fluid having temperature-dependent properties and Sinha et al.[6] Peristaltic transport of MHD flow and heat transfer in an asymmetric channel: effects of variable viscosity, velocity-slip and temperature jump and Hayat et al. [28] Influence of convective conditions in radiative peristaltic flow of pseudoplasticnanofluid in a tapered asymmetric channel.

In this paper we will studies heat and mass transfer in asymmetric tapered channels during peristaltic transport of a magnetohydrodynamic fluid having temperature-dependent properties through porous medium, where wavelength of the peristaltic flow is long and the Reynolds number is small. The equations for the momentum and energy have been linearized on the basis of these considerations. Expressions for the stream function, velocity, pressure gradient and temperature have been obtained. Pumping characteristics of the peristaltic flow and the trapping phenomenon have been discussed. Numerical results of different physical parameters in the through the peristaltic transport in tapered channel of the MHD fluid have been obtained by using the software MATHEMATICA.

2. Mathematical Formulation

In the present study, we consider the flow of an incomp-ressible magnetohydrodynamic (MHD) nanofluid in a two-dimensional tapered asymmetric channel of width $(d_1 + d_2)$ through a porous space (see Fig.(1)) under the effect of heat and mass transfer. Wave speed of peristaltic waves is denoted by$c$. Here$\tilde{X}-$axis is taken along the length of channel and$\tilde{Y}-$axis transverse to it. A uniform magnetic field$B = (0, B_0, 0)$is applied. The induced magnetic field is neglected by assuming a very small magnetic Reynolds number. Also the electric field is taken absent. We choose$Y = \tilde{H}_1$and$Y = \tilde{H}_2$as the right side and the left walls respectively. The geometry of the wall surfaces is given as follows:

$$\tilde{Y} = \tilde{H}_1(\tilde{X}, t) = d_1 + \acute{m}\tilde{X} + b_1 Cos\left[\frac{2\pi}{\lambda}(\tilde{X} - c\acute{t})\right], \quad (1)$$

$$\tilde{Y} = \tilde{H}_2(\tilde{X}, t) = -d_2 - \acute{m}\tilde{X} - b_2 Cos\left[\frac{2\pi}{\lambda}(\tilde{X} - c\acute{t}) + \phi\right]. \quad (2)$$

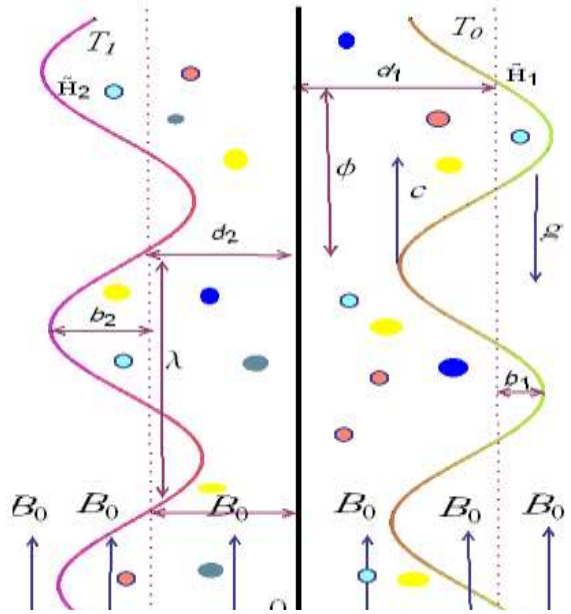

Figure 1: Geometry of the tapered asymmetric channel

Where $(d_1), (d_2)$ the channel width, (b_1) and (b_2) are the amplitudes of right and left walls respectively, (c) is the phase speed of the wave, $\acute{m}(\ll 1)$ is the non-uniform parameter, (λ) is the wave length, $(\acute{t})$ the time, the phase difference (ϕ) varies in the range$0 \le \phi \le \pi, \phi =$ 0corresponds to symmetric channel with waves out of phase i.e. both walls move towards outward or inward simultaneously and further $b_1, b_2, d_1, d_2$and ϕ satisfy the following condition at the inlet of divergent channel

$$b_1^2 + b_2^2 + 2b_1 b_2 Cos\,\phi \le (d_1 + d_2)^2 \quad (3)$$

Here we assume the fluid to be electrically conducting in the presence of a uniform inclined magnetic field $B = (0, B_0, 0)$. To calculate the Lorentz force we will apply a magnetic field just in $\tilde{Y} - direction$ and then we study the effect of it on the fluid flow.

3. Governing Equations

Based on the consideration made above, the governing equations that describe the flow in the present study are given by

$$\frac{\partial \tilde{U}}{\partial \tilde{X}} + \frac{\partial \tilde{V}}{\partial \tilde{Y}} = 0 \quad (4)$$

$$\rho\left[\frac{\partial \tilde{U}}{\partial \acute{t}} + \tilde{U}\frac{\partial \tilde{U}}{\partial \tilde{X}} + \tilde{V}\frac{\partial \tilde{U}}{\partial \tilde{Y}}\right] = -\frac{\partial \tilde{P}}{\partial \tilde{X}} + 2\frac{\partial}{\partial \tilde{X}}\left[\tilde{\mu}(\tilde{T})\frac{\partial \tilde{U}}{\partial \tilde{X}}\right] + \frac{\partial}{\partial \tilde{Y}}\left[\tilde{\mu}(\tilde{T})\left(\frac{\partial \tilde{V}}{\partial \tilde{X}} + \frac{\partial \tilde{U}}{\partial \tilde{Y}}\right)\right] - \acute{\sigma}B_0^2\tilde{U} + \rho g\,\alpha_1(\tilde{T} - T_0) - \frac{\tilde{\mu}(\tilde{T})}{K_0} \quad (5)$$

$$\rho\left[\frac{\partial \tilde{V}}{\partial t}+\tilde{U}\frac{\partial \tilde{V}}{\partial \tilde{X}}+\tilde{V}\frac{\partial \tilde{V}}{\partial \tilde{Y}}\right]=-\frac{\partial \tilde{P}}{\partial \tilde{Y}}+2\frac{\partial}{\partial \tilde{Y}}\left[\tilde{\mu}(\tilde{T})\frac{\partial \tilde{V}}{\partial \tilde{X}}\right]$$
$$+\frac{\partial}{\partial \tilde{X}}\left[\tilde{\mu}(\tilde{T})\left(\frac{\partial \tilde{V}}{\partial \tilde{X}}+\frac{\partial \tilde{U}}{\partial \tilde{Y}}\right)\right]-\frac{\tilde{\mu}(\tilde{T})}{K_0}\tilde{V} \quad (6)$$

$$\rho C_p\left[\frac{\partial \tilde{T}}{\partial t}+\tilde{U}\frac{\partial \tilde{T}}{\partial \tilde{X}}+\tilde{V}\frac{\partial \tilde{T}}{\partial \tilde{Y}}\right]=k+\frac{\partial \tilde{q}_r}{\partial \tilde{Y}}+Q_0 \quad (7)$$

Where the Eq.(4) ensures the conservation of mass, while Eqs.(5) and (6) are the momentum conservation equations and $\tilde{T}$ is the temperature at any point $(\tilde{X},\tilde{Y})$ of the fluid mass in motion.

By using Rosseland approximation (cf.[7]), the relative heat flux is given by

$$\tilde{q}_r=\frac{4\sigma^*}{3k^*}\frac{\partial \tilde{T}^4}{\partial \tilde{Y}} \quad (8)$$

Under the consideration that the temperature difference within the fluid mass that flows is sufficiently small, using Taylor expansion and neglecting higher-order terms, we can write

$$\tilde{T}^4=4T_0{}^3\tilde{T}-3T_0{}^4 \quad (9)$$

Now, for $\tilde{U}$ and $\tilde{V}$ be the respective velocity components along $\tilde{X}$ and $\tilde{Y}$ directions in the fixed fram, respectively. For the unsteady two-dimensional flow, the velocity components may be written $\tilde{\boldsymbol{V}}=\left(\tilde{U}(\tilde{X},\tilde{Y}),\tilde{V}(\tilde{X},\tilde{Y}),0\right)$.

The temperature function may be written $T=T(\tilde{X},\tilde{Y})$.
The appropriate boundary conditions comprising wall slip and convective boundary conditions are given as follows:

$$\tilde{U}+\beta\frac{\partial \tilde{U}}{\partial \tilde{y}}=0\,,\quad \tilde{T}=T_1 \quad at\quad \tilde{Y}=\tilde{H}_1 \quad (10)$$

$$\tilde{U}-\beta\frac{\partial \tilde{U}}{\partial \tilde{y}}=0\,,\quad \tilde{T}=T_0 \quad at\quad \tilde{Y}=\tilde{H}_2 \quad (11)$$

If we introduce the wave frame having coordinates $(\tilde{x},\tilde{y})$ which travel in the $\tilde{x}-direction$ with the same wave velocity (c). Then the unsteady flow in the laboratory frame $(\tilde{X},\tilde{Y})$ can be treated as steady. The coordinates and velocities in the two frames are related by

$$\left.\begin{aligned}&\tilde{x}=\tilde{X}-c\tilde{t}\,,\tilde{y}=\tilde{Y},\tilde{u}(\tilde{x},\tilde{y})=\tilde{U}(\tilde{X},\tilde{Y},\tilde{t})-c\,,\\&\tilde{v}(\tilde{x},\tilde{y})=\tilde{V}(\tilde{X},\tilde{Y},\tilde{t}),\\&\tilde{p}(\tilde{x},\tilde{y})=\tilde{P}(\tilde{X},\tilde{Y},\tilde{t})\,,T=\tilde{T}\end{aligned}\right] \quad (12)$$

Where $\tilde{u},\tilde{v}$ are the velocity components in the wave frame $(\tilde{x},\tilde{y})$.
Using the transformations in Eq.(12) into constitutive relations (4)-(7) we have the following form.

$$\frac{\partial(\tilde{u}+c)}{\partial(\tilde{x}+c\tilde{t})}+\frac{\partial \tilde{v}}{\partial \tilde{y}}=0 \quad (13)$$

$$\rho\left[\frac{\partial(\tilde{u}+c)}{\partial t}+(\tilde{u}+c)\frac{\partial(\tilde{u}+c)}{\partial(\tilde{x}+c\tilde{t})}+\tilde{v}\frac{\partial(\tilde{u}+c)}{\partial \tilde{y}}\right]$$
$$=-\frac{\partial \tilde{p}}{\partial(\tilde{x}+c\tilde{t})}+2\frac{\partial}{\partial(\tilde{x}+c\tilde{t})}\left[\tilde{\mu}(T)\frac{\partial(\tilde{u}+c)}{\partial(\tilde{x}+c\tilde{t})}\right]$$
$$+\frac{\partial}{\partial \tilde{y}}\left[\tilde{\mu}(T)\left(\frac{\partial \tilde{v}}{\partial(\tilde{x}+c\tilde{t})}+\frac{\partial(\tilde{u}+c)}{\partial \tilde{y}}\right)\right]$$
$$-\acute{\sigma}B_0^2\tilde{U}+\rho g\alpha_1(T-T_0)-\frac{\tilde{\mu}(T)}{K_0}(\tilde{u}+c) \quad (14)$$

$$\rho\left[\frac{\partial \tilde{v}}{\partial t}+(\tilde{u}+c)\frac{\partial \tilde{v}}{\partial(\tilde{x}+c\tilde{t})}+\tilde{v}\frac{\partial \tilde{v}}{\partial \tilde{y}}\right]$$
$$=-\frac{\partial \tilde{p}}{\partial \tilde{y}}+2\frac{\partial}{\partial \tilde{y}}\left[\tilde{\mu}(T)\frac{\partial \tilde{v}}{\partial \tilde{y}}\right]$$
$$+\frac{\partial}{\partial(\tilde{x}+c\tilde{t})}\left[\tilde{\mu}(T)\left(\frac{\partial \tilde{v}}{\partial(\tilde{x}+c\tilde{t})}+\frac{\partial(\tilde{u}+c)}{\partial \tilde{y}}\right)\right]-\frac{\tilde{\mu}(T)}{K_0}\tilde{v} \quad (15)$$

$$\rho C_p\left[(\tilde{u}+c)\frac{\partial T}{\partial(\tilde{x}+c\tilde{t})}+\tilde{v}\frac{\partial T}{\partial \tilde{y}}\right]=k\left[\frac{\partial^2 T}{\partial(\tilde{x}+c\tilde{t})^2}+\frac{\partial^2 T}{\partial \tilde{y}^2}\right]$$
$$+\frac{\partial \tilde{q}_r}{\partial \tilde{y}}+Q_0 \quad (16)$$

We will introduce the following new quantities

$$\left.\begin{aligned}&x=\frac{\tilde{x}}{\lambda}\,,\ y=\frac{\tilde{y}}{d_1}\,,\ t=\frac{c\tilde{t}}{\lambda}\,,\ u=\frac{\tilde{u}}{c}\,,\\&v=\frac{\lambda\tilde{v}}{d_1 c}\,,\ \delta=\frac{d_1}{\lambda}\,,\theta=\frac{T-T_0}{\Delta T}\,,\\&h_1(x)=\frac{\tilde{H}_1(\tilde{x})}{d_1}\,,h_2(x)=\frac{\tilde{H}_2(\tilde{x})}{d_1}\,, \quad (17)\\&\mu(\theta)=\frac{\tilde{\mu}(T)}{\mu_0}\,,p=\frac{{d_1}^2\tilde{p}}{\lambda\mu_0 c}\,,m=\frac{\acute{m}\lambda}{d_1}\,,\\&K=\frac{K_0}{{d_1}^2}\,,\ a=\frac{b_1}{d_1}\,,\ b=\frac{b_2}{d_1}\,,\beta_1=\frac{\beta}{d_1}\,,\\&Gr=\frac{\rho g\alpha_1(\Delta T){d_1}^2}{c\mu_0}\,,\ Nr=\frac{16}{3}\frac{\sigma^*{T_0}^2}{k^*k}\,,\ \beta=\frac{Q_0{d_1}^2}{k(\Delta T)}\,,\\&M=\sqrt{\frac{\acute{\sigma}}{\mu_0}}d_1B_0\,,Pr=\frac{\mu_0 C_p}{\kappa}\,,Re=\frac{\rho c d_1}{\mu_0}\,.\end{aligned}\right]$$

Where (x) is the non-dimensional axial coordinate, (y) is the non-dimensional transverse coordinate, (t) is the dimensionless time, (u) and (v) are non-dimensional axial and transverse velocity components respectively, (p) is the dimensionless pressure, (a) and (b) are amplitudes of upper and lower walls, (δ) is the wave number, (m) is the non-uniform parameter, (θ) is the dimensionless temperature, $(\Delta T=T_1-T_0)$ denote the temperature difference, $(\boldsymbol{\rho})$the density of nano-particles, $(\kappa)$the thermal conductivity of fluid, (K) is the Darcy number, $(K_0)$the permeability parameter, (β) is the heat source/sink parameter, the velocity-slip parameter (β_1), the Grashof number (Gr), (Nr) is the thermal radiation parameter, (Pr) is the Prandtl number, (M) is the Hartmann number and (Re) is the Reynolds number.

Using the above dimensionless quantities of Eq.(17) and the wave length approximation($\delta\ll 1$)and the definition of stream function ($u=\frac{\partial v}{\partial y}, v=-\frac{\partial v}{\partial x}$).

$$\frac{\partial p}{\partial x}=\frac{\partial}{\partial y}\left(\mu(\theta)\frac{\partial^2\psi}{\partial y^2}\right)-M^2\left(\frac{\partial \psi}{\partial y}+1\right)$$
$$+Gr.\theta-\frac{1}{\kappa}\mu(\theta)\left(\frac{\partial \psi}{\partial y}+1\right) \quad (18)$$

$$\frac{\partial p}{\partial y}=0 \quad (19)$$

Although in most previous studies of fluid mechanical problems for the sake of simplicity of the analysis, fluid viscosity has been taken to be constant, in many processes viscosity is a function of temperature. Keeping this in mind, in the present study temperature dependence of fluid viscosity has been accounted for by treating it as an exponential function of temperature. Let us take ($\mu(\theta)=e^{-\alpha\theta}$), where (α) is the Reynolds model viscosity parameter, which is a constant. For $\alpha\ll 1$, neglecting squares and higher powers of (α), we write

$$\mu(\theta)=1-\alpha\theta \quad for\ \alpha\ll 1. \quad (21)$$

From Eq.(19) shows that (p) is not a function of (y) of the non-dimensional axial coordinate y. Accordingly we get the following

$$\frac{\partial p}{\partial x}=\frac{\partial}{\partial y}\left((1-\alpha\theta)\frac{\partial^2\psi}{\partial y^2}\right)-M^2\left(\frac{\partial\psi}{\partial y}+1\right)+Gr.\theta-\frac{1}{K}(1-\alpha\theta)\left(\frac{\partial\psi}{\partial y}+1\right) \quad (22)$$

$$0=\frac{\partial^2 p}{\partial y\partial x}=(1-\alpha\theta)\frac{\partial^4\psi}{\partial y^4}-2\alpha\frac{\partial\theta}{\partial y}\frac{\partial^3\psi}{\partial y^3}-\alpha\frac{\partial^2\theta}{\partial y^2}\frac{\partial^2\psi}{\partial y^2}-\left(N^2-\frac{1}{K}\alpha\theta\right)\frac{\partial^2\psi}{\partial y^2}+\frac{\alpha}{K}\frac{\partial\theta}{\partial y}\left(\frac{\partial\psi}{\partial y}+1\right)+Gr\frac{\partial\theta}{\partial y} \quad (23)$$

Where $N^2=M^2+\frac{1}{K}$

4. Rate of Volume Flow

The instantaneous volume flow rate in the fixed frame of reference $(\tilde{X},\tilde{Y})$ is given by

$$Q=\int_{\tilde{H}_2(\tilde{X},t')}^{\tilde{H}_1(\tilde{X},t')}\tilde{U}(\tilde{X},\tilde{Y},t')\,d\tilde{Y} \quad (24)$$

We replace Eq.(12) in Eq.(24) to obtain

$$Q=\tilde{q}+c\left[\tilde{H}_1(\tilde{X},t)-\tilde{H}_2(\tilde{X},t)\right] \quad (25)$$

Where in the wave frame, the expression for the volumetric flow rate ($\tilde{q}$) at the following

$$\tilde{q}=\int_{\tilde{H}_2(\tilde{X},t)}^{\tilde{H}_1(\tilde{X},t')}\tilde{u}(\tilde{x},\tilde{y},t')d\tilde{y} \quad (26)$$

The time-mean flow over a period of time T ($=\frac{\lambda}{c}$) at fixed position x is defined as

$$\tilde{Q}=\frac{1}{T}\int_0^T Q\,dt' \quad (27)$$

We replace Eq.(25) in to Eq.(27) and integrating, we get

$$\tilde{Q}=\tilde{q}+c[d_1+d_2]+2c\acute{m}\tilde{x} \quad (28)$$

Now, from the Eqs.(1), (2) and Eq.(28) we get

$$\tilde{Q}=\tilde{q}-cb_1Cos\left[\frac{2\pi}{\lambda}(\acute{X}-c\acute{t})\right]-cb_2Cos\left[\frac{2\pi}{\lambda}(\acute{X}-c\acute{t})+\phi\right], \quad (29)$$

Let F be a dimensionless mean flows and $\tilde{\Theta}$ is the dimensionless time-mean flows where

$$F=\frac{\tilde{q}}{cd_1}and\tilde{\vartheta}=\frac{\tilde{Q}}{cd_1} \quad (30)$$

By the Eqs.(17), (28), (29) and(30) and ($d=\frac{d_2}{d_1}$), we get

$$\tilde{\Theta}=F+1+d+2mx \quad (31)$$

Where

$$F=\int_{h_2(x)}^{h_1(x)}\frac{\partial\psi}{\partial y}\,dy=\psi\left(h_1(x)\right)-\psi\left(h_2(x)\right) \quad (32)$$

Note that$h_1(x)$and$h_2(x)$represent two non-dimensional quantities such that

$$h_1(x)=1+m(t+x)+aCos[2\pi x] \quad (33)$$

$$h_2(x)=-d-m(t+x)-bCos[2\pi x+\phi] \quad (34)$$

In which($a=\frac{b_1}{d_1}$) and ($b=\frac{b_2}{d_1}$), and from there Eq.(3) takes the form of

$$a^2+b^2+2ab\,Cos\,\phi\le(1+d)^2 \quad (35)$$

The Eqs.(10), (11) and by using Eqs.(12), (17), the boundary conditions for the dimensionless stream function and the temperature in the wave frame are

$$\left.\begin{aligned}\psi=\frac{F}{2},\ \frac{\partial\psi}{\partial y}+\beta_1\frac{\partial^2\psi}{\partial y^2}=-1,\theta=1\ aty=h_1\\ \psi=-\frac{F}{2},\ \frac{\partial\psi}{\partial y}-\beta_1\frac{\partial^2\psi}{\partial y^2}=-1,\theta=0\ aty=h_2\end{aligned}\right] \quad (36)$$

5. Solution of the Temperature Equation

Exact solution of the temperature Eq.(20) satisfying the boundary conditions (36) given by

$$\theta=C1+yC2-\frac{y^2\beta}{2(1+Nr)} \quad (37)$$

6. Perturbed System and Perturbation Solutions

Although solution the Eq.(20) that depict the heat of a peristaltic motion of the fluid mass under consideration could be achieved, but has not been possible determination of a similar solution for Eq.(18).So we will find a solution by to one of the approximate numerical methods, which is the perturbation method to solve the momentum equation. We assume that the dimensionless quantities, the stream function (ψ) and the flow rate (F) can be expanded in powers of $\alpha(\alpha\ll1)$ as follows:

$$\left.\begin{aligned}P=P_0+\alpha P_1+\alpha^2P_2+\cdots,\\ \psi=\psi_0+\alpha\psi_1+\alpha^2\psi_2+\cdots,\\ F=F_0+\alpha F_1+\alpha^2F_2+\cdots\ .\end{aligned}\right] \quad (38)$$

Compensation for Eq.(38) into Eq.(22) and Eq.(23) and boundary conditions (41) and then equating the like powers of (α)we get:

7. Perturbed Systems

7.1 Zeroth- Order System

$$\left.\begin{aligned}\frac{\partial p_0}{\partial x}=\frac{\partial^3\psi_0}{\partial y^3}-N^2\left(\frac{\partial\psi_0}{\partial y}+1\right)+Gr.\theta \quad (39)\\ \frac{\partial^4\psi_0}{\partial y^4}-N^2\frac{\partial^2\psi_0}{\partial y^2}+Gr\frac{\partial\theta}{\partial y}=0\end{aligned}\right] \quad (40)$$

With corresponding boundary conditions

$$\left.\begin{aligned}\psi_0=\frac{F_0}{2},\frac{\partial\psi_0}{\partial y}+\beta_1\frac{\partial^2\psi_0}{\partial y^2}=-1,\theta=1\ at\ y=h_1\\ \psi_0=-\frac{F_0}{2},\frac{\partial\psi_0}{\partial y}-\beta_1\frac{\partial^2\psi_0}{\partial y^2}=-1,\theta=0\ at\ y=h_2\end{aligned}\right] \quad (41)$$

7.2 First- Order System

$$\frac{\partial p_1}{\partial x} = \frac{\partial^3 \psi_1}{\partial y^3} - \theta \frac{\partial^3 \psi_0}{\partial y^3} - \frac{\partial \theta}{\partial y}\frac{\partial^2 \psi_0}{\partial y^2} - N^2 \frac{\partial \psi_1}{\partial y} + \frac{\theta}{k}\left(\frac{\partial \psi_0}{\partial y} + 1\right) \quad (42)$$

$$\frac{\partial^4 \psi_1}{\partial y^4} - \theta \frac{\partial^4 \psi_0}{\partial y^4} - 2\frac{\partial \theta}{\partial y}\frac{\partial^3 \psi_0}{\partial y^3} - \frac{\partial^2 \theta}{\partial y^2}\frac{\partial^2 \psi_0}{\partial y^2} - N^2 \frac{\partial^2 \psi_1}{\partial y^2} + \frac{\theta}{k}\frac{\partial^2 \psi_0}{\partial y^2} + \frac{1}{k}\frac{\partial \theta}{\partial y}\left(\frac{\partial \psi_0}{\partial y} + 1\right) = 0 \quad (43)$$

With corresponding boundary conditions

$$\left.\begin{aligned} \psi_1 = \frac{F_1}{2}, \frac{\partial \psi_1}{\partial y} + \beta_1 \frac{\partial^2 \psi_1}{\partial y^2} = 0, \theta = 1 \text{ at } y = h_1 \\ \psi_1 = -\frac{F_1}{2}, \frac{\partial \psi_1}{\partial y} - \beta_1 \frac{\partial^2 \psi_1}{\partial y^2} = 0, \theta = 0 \text{ at } y = h_2 \end{aligned}\right\} \quad (44)$$

8. Perturbation Solutions

8.1 Zeroth- Order Solution

The solution of Eq. (40) satisfying the boundary conditions (41) given by

$$\psi_0 = C5 + y\,C6 + \frac{2e^{-yN}C3 + 2e^{yN}C4 + C2y^2Gr - \frac{y^3 \beta Gr}{3(1+Nr)}}{2N^2} \quad (45)$$

8.2 First- Order Solution

By the zeroth-order solution Eq.(45) and the Eq.(43) and then solving the resulting system with the corresponding boundary conditions (44), we get

$$\begin{aligned} \psi_1 = {} & C9 + y\,C10 + \frac{1}{120kN^4} e^{-yN}(45(24C2B6e^{yN}y^2 \\ & + A3(5B3 + e^{yN}(5B4e^{yN} + 16y^2(B5 + 2B6y)))) \\ & + 105(B3 - B4e^{2yN})(C2 + 2A3y)N + (30C1(5B3 \\ & + e^{yN}(5B4e^{yN} + 4y^2(B5 + B6y))) \\ & + A3(-15B3(k - 6y^2) \\ & + e^{yN}(15B4e^{yN}(-k + 6y^2) \\ & + 4y^2(15B5(-4k + y^2) \\ & + 2y(5 + 5C6 - 90B6k + 9B6y^2)))) \\ & + 10(C2y(9B3 + e^{yN}(9B4e^{yN} + y(6 + 6C6 \\ & + 8B5y + 9B6(-8k + y^2)))) \\ & + 12k(C7 + e^{2yN}C8)))N^2 \\ & + 5(B3 - B4e^{2yN})(9C2k + 12C1y \\ & - 6A3ky + 6C2y^2 + 4A3y^3)N^3 \\ & - 30(B3 + B4e^{2yN})k(5C1 + y(C2 + A3y))N^4 \\ & - 10(B3 - B4e^{2yN})ky(6C1 \\ & + y(3C2 + 2A3y))N^5)(46) \end{aligned}$$

Now by Eq.(39), (42) the pressure rise (Δp) per wavelength and the walls shear stress can be obtained by the formula

$$\Delta p = \int_0^1 \frac{\partial p}{\partial x}\, dx \quad (47)$$

And the shear stress on the two walls of the channel can be defined as follows:

$$\tau_{rw} = -\left(\frac{\partial u}{\partial y}\right)_{y=h1} \quad (48)$$

And

$$\tau_{lw} = -\left(\frac{\partial u}{\partial y}\right)_{y=h2} \quad (49)$$

Where the symbols (τ_{rw}) and (τ_{lw}) stand for the wall shear stress at the right and left side walls respectively.

9. Numerical Results and Discussion

In this paper, the graphical description of various parameters on flow of pseudoplastic nanofluids in the tapered asymmetric channel. Particularly the results of pressure gradient distribution, average pressure rise, axial velocity, temperature distribution, shear stress at the right side and the left side walls and stream function are recorded in terms of plots and then discussed physically. **MATHEMATICAL** software is used to find out numerical results and illustration.

9.1. The Pressure gradient distribution

In this paper, Figs.(2)-(5) shows the pressure gradient ($\frac{dp}{dx}$) for different values of the Hartman number (M), the velocity-slip parameter (β_1), the thermal radiation parameter (Nr) and mean flow rate (Q) and the values of y and t are fixed at $y = 0.2$ and $t = 3$. The Figs.(2) and (4) and (5) shows that increase in (M) and (Nr) and (Q) results in the decrease of ($\frac{dp}{dx}$).While opposite behavior on Fig.(3) is observed with an increase in (β_1) led to ($\frac{dp}{dx}$) is increasing.

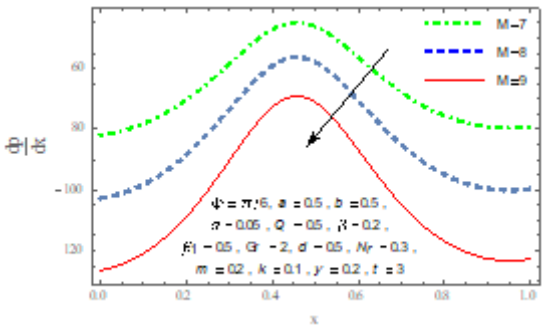

Figure 2: Variation of pressure gradient $\frac{dp}{dx}$with different values of$M$

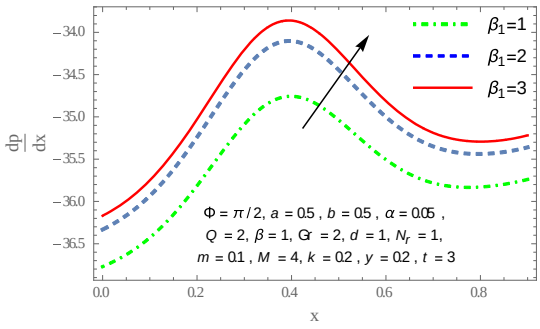

Figure 3: Variation of pressure gradient $\frac{dp}{dx}$with different values ofβ_1

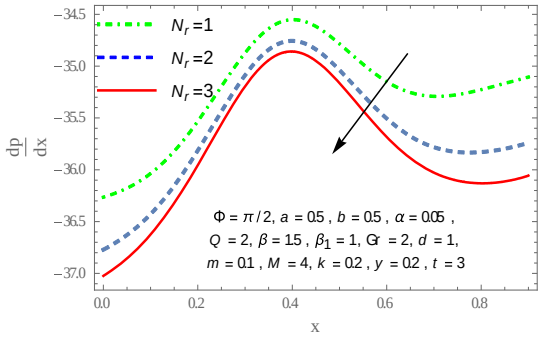

Figure 4: Variation of pressure gradient $\frac{dp}{dx}$ with different values of Nr

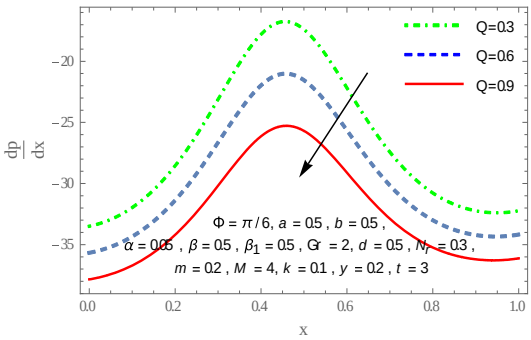

Figure 5: Variation of pressure gradient $\frac{dp}{dx}$ with different values of Q

9.2 Pumping Characteristics

Figs.(6)-(9) show the plots of average pressure rise (Δp) against mean flow rate (Q), for various physical parameters including the thermal radiation parameter (Nr) and Hartman number (M) and the Grashof number (Gr) and the heat source/sink parameter (β) on the average pressure rise (Δp). It may be seen that all the plots in the figures are of rectilinear nature. In these plots, the upper left-hand Quadrant (**I**)(Q<0, Δp>0) represents the region of retrograde pumping region. Quadrant (**II**) (Q>0, Δp>0) there is no flow region. Quadrant (**III**) (Q>0, Δp<0) which Q>0 (positive pumping) and Δp<0 (favorable pressure gradient) is marked as the co-pumping region (or augmented flow).Quadrant (**IV**)(Q<0, Δp<0) represents peristaltic pumping. The pumping rate decreases with an increase in (Nr) (see Fig.(6)) in the co-pumping region (Q>0, Δp<0).Fig.(7)Graph shows that the pumping rate decrease in the co-pumping region ($Q > 0, \Delta p < 0$)with an increase in (M). One can also observe in Fig.(8) that the pumping rate increased in the co-pumping region with increasing in (Gr). Fig.(9) shows the impact of (β) on average pressure rise (Δp). We observed from the graph that in co-pumping region ($Q > 0, \Delta p < 0$), the pumping rate increase with enhances of (β).

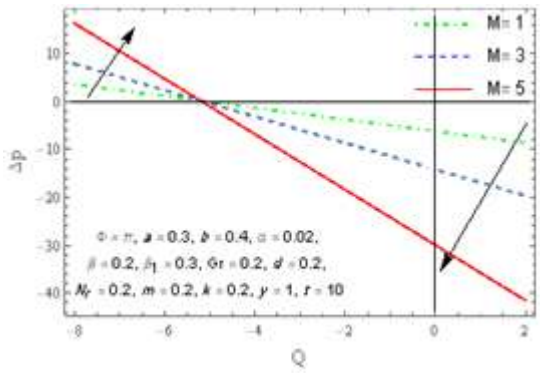

Figure 6: Pressure rise Δp versus time-averaged flow rate Q for$M$

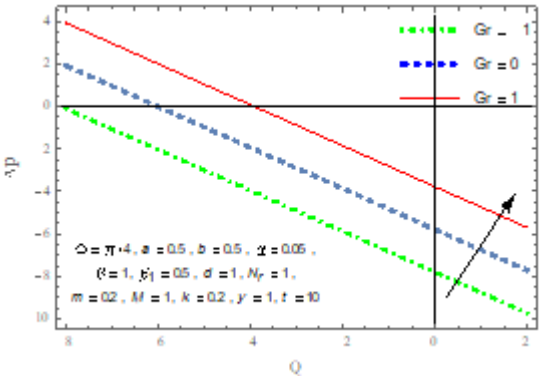

Figure 7: Pressure rise Δp versus time-averaged flow rate Q for Nr

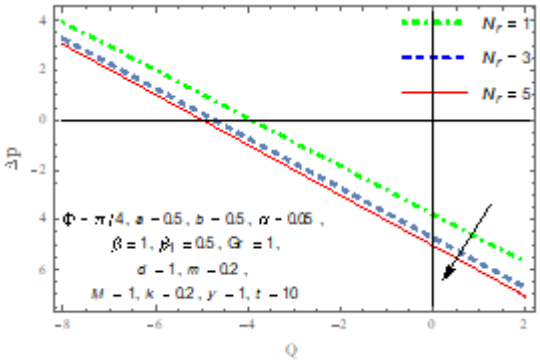

Figure 8: Pressure rise Δp versus time-averaged flow rate Q for Gr

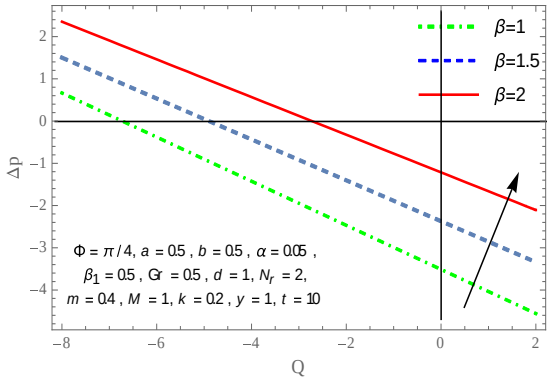

Figure 9: Pressure rise Δp versus time-averaged flow rate Q for β

9.3 Velocity Profile

To see the effects of a change in the values of the Grashof number (Gr), Hartmann number (M), the thermal radiation parameter (Nr), mean flow rate (Q), and the Reynolds model

viscosity parameter (α) on the velocity profile (u). For the sake of generality of the problem, the graphs are sketched in Figs.(10)-(14) at the fixed values of $x = 3$ and $t = 0.3$.The behavior of velocity profile is parabola as seen through figures. The velocity profile with the Grashof number (Gr) is plotted in Fig.(10). We observed from the graph if there is a gradual increase in (Gr), the velocity is gradually increases up to a certain point (point of inflexion which is (-0.58, 0.62)), after which the trend is reversed in this case when the value of (Gr) is increased, the velocity gradually decreases. In both the cases the magnitude of the velocity merges to a fixed value at the wall. The Fig.(11) gives an idea of the change in velocity distribution, Initially the velocity is decreases with increasing of Hart-mann number (M) up to a point which(-1.5, 0.46), Then the situation is reflected where the velocity distribution increasing with increasing of (M) after then gradually decreasing to other point (2.4, 0.48) the situation is reflected here too, after crossing the point of inflexion the magnitudes of the velocity converge to a particular value at the wall of the asymmetric channel boundaries. From Fig.(12) the axial velocity (u) increases with an increase in the thermal radiation parameter (Nr) at the core part of the channel. However opposite behavior is observed near channel boundaries. We observed from Fig.(13) which depicts that the axial velocity (u) decreases with an increase in the mean flow rate parameter (Q) at the core part of the channel while we note that the magnitude of (u)is a matches exactly at the boundaries. We observed from Fig.(14) the velocity profile for the Reynolds model viscosity parameter (α), Initially the velocity is increases with increasing of (α) up to a point which (-0.75, 0.63), Then the situation is reflected where the velocity is decreasing with increasing of (α) after then to other point (2.4, 0.6) the situation is reflected here.

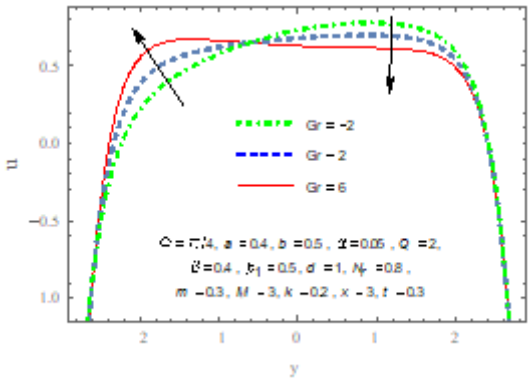

Figure 10: Axial velocity u versus$y$-direction for different values Gr

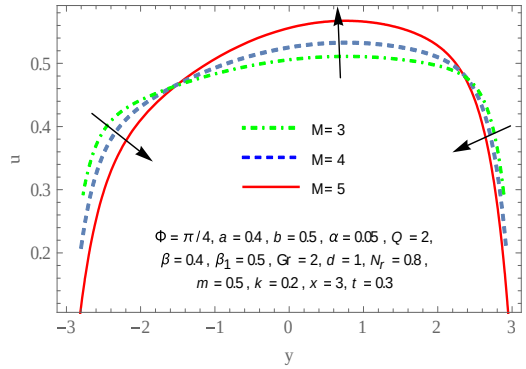

Figure 11: Axial velocity u versus y-direction for different values M

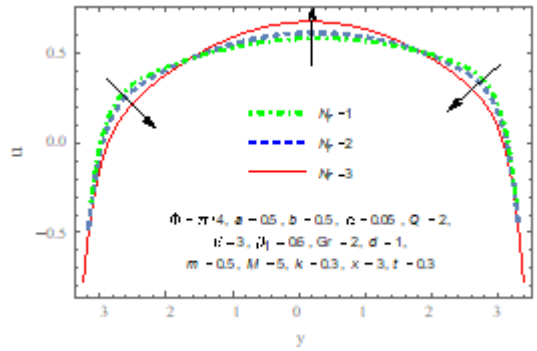

Figure 12: Axial velocity u versus y-direction for different values Nr

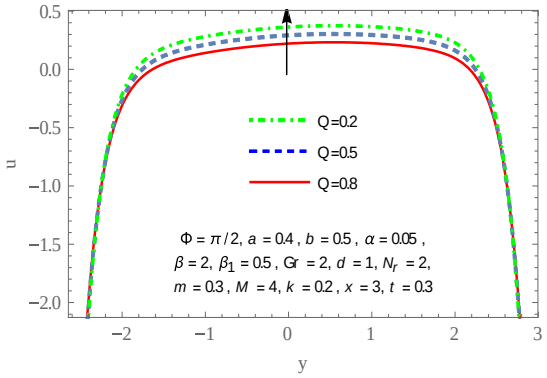

Figure 13: Axial velocity u versus y-direction for different values Q

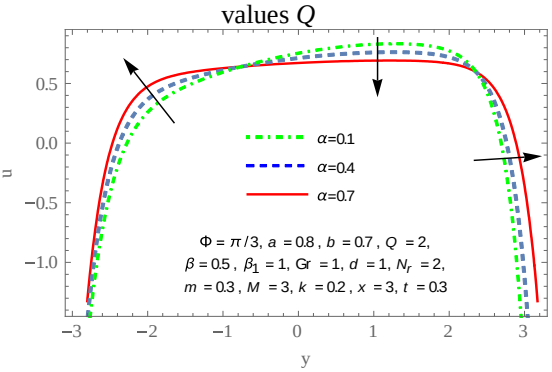

Figure 14: Axial velocity u versus y-direction for different values α

9.4. Temperature distribution

The Figs.(15)-(18) are presents the change in the temperature distribution during the peristaltic motion of the fluid for the fixed values of $x = 0.2$ and $t = 0.3$. Fig.(15) shows that temperature rises, as the value of the heat source/sink parameter (β) increases, while the Fig.(16) is indicate an opposite trend, when increasing of the thermal radiation parameter (Nr) we note that the magnitude of temperature decreases. This figure reveals that the temperature profile is greatly affected by thermal radiation. We observed from Fig.(17) shows that the phase difference (ϕ) does have an appreciable impact on the temperature distribution and that thermal boundary layer decreases with increase in phase difference and we can note that the initial point is gradually shifted towards the central region of the channel with a rise in the phase difference. Fig.(18) it is seen that the temperature distribution enhances with an increase in (m).

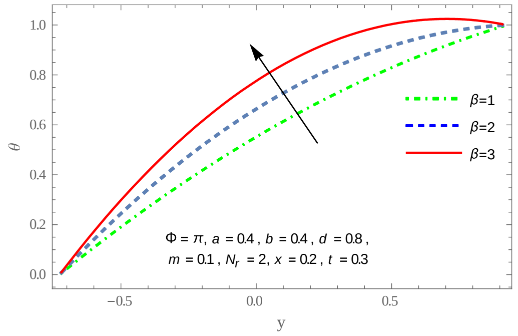

Figure 15: Temperature distributionθ for different values β

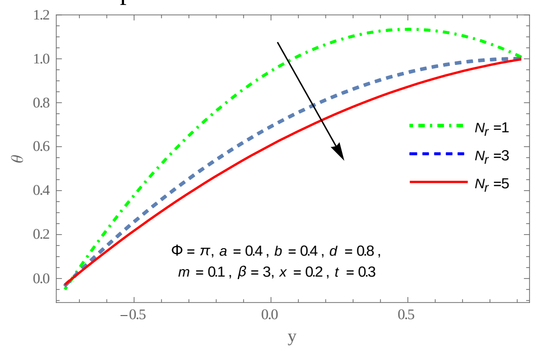

Figure 16: Temperature distributionθ for different values Nr

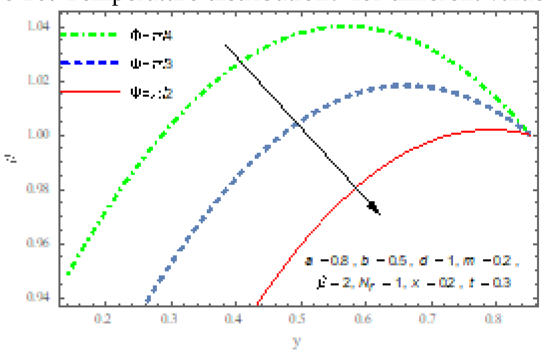

Figure 17: Temperature distributionθ for different values $\boldsymbol{\phi}$

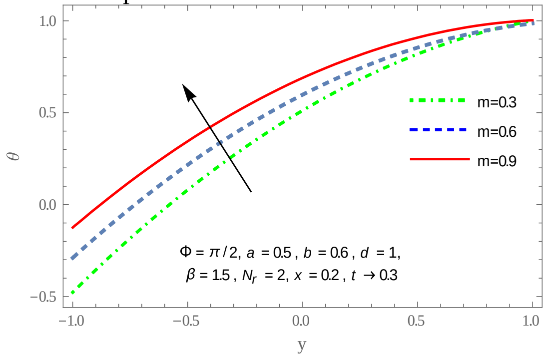

Figure 18: Temperature distributionθ for different values m

9.5. Wall shear stress

The variation of wall shear stress (τ) versus Grashof number (Gr) on both the right and left walls of the asymmetric channel. The Fig.(19) shows that decrease of the shear stress for right wall (τ_{lw}) with increasing of Hartmann number (M), but the opposite in Fig. (20) which shows that (τ_{lw}) increasing with increase in the slip velocity (β_1). Fig.(21) shows that increase shear stress (τ_{uw}) on the left wall with enhance Hartmann number (M), but the opposite in Fig. (22) with slip velocity (β_1).

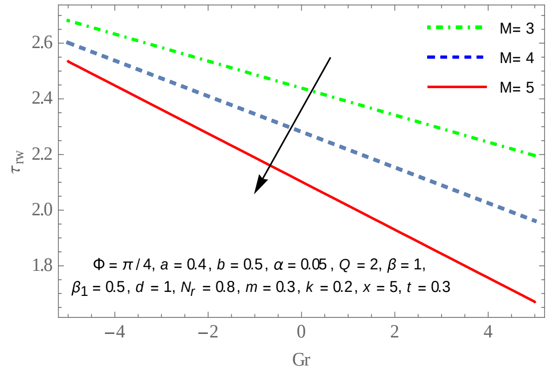

Figure 19: Variation of shear stressτ_{rw} for different values of M

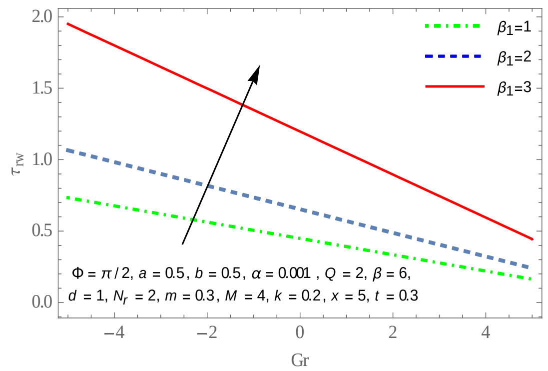

Figure 20: Variation of shear stressτ_{rw} for different values of β_1

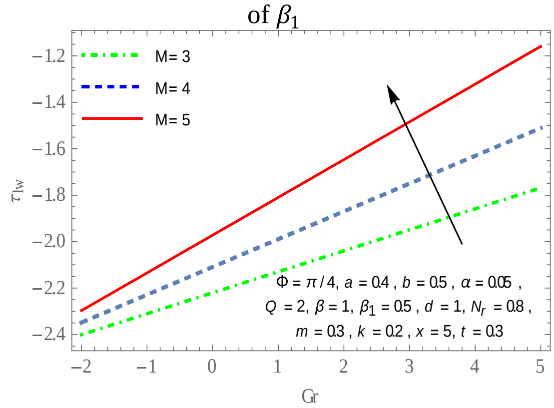

Figure 21: Variation of shear stressτ_{lw} for different values of M

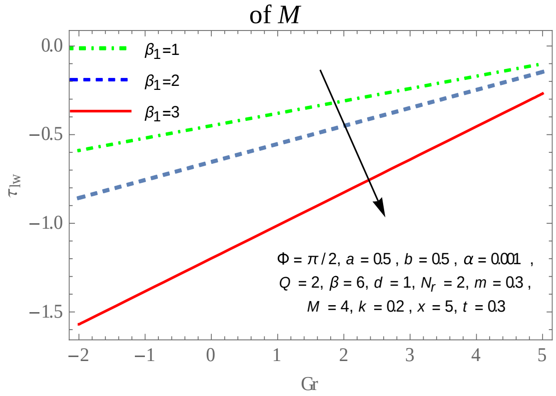

Figure 22: Variation of shear stressτ_{lw} for different values of β_1

10. Trapping

The trapping is an interesting phenomenon in peristalsis. The shape of streamlines is similar to the wave shape traveling

across the channel walls. These streamlines split and enclose a bolus that moves along with the wave. The Figs.(23)-(29) at fixed values of $t = 0.3$ indicate the behavior of parameters (M, Gr, Nr, Q, ϕ, α, β_1) in the stream function. Fig.(23) shows that the size of trapped bolus is decreases with an increase Hartmann number (M).From Fig.(24) we observe the difference in the values of the Grashof number (Gr), which have a slight effect on a stream function. Fig.(25) is plotted to study the behavior of the thermal radiation parameter (Nr), this figure shows that the size of bolus is no effected on stream function. The effect of the mean flow rate (Q) on the streamlines is observed in Fig.(26).We found that with the ascending values of (Q), the trapping bolus increases in size. We observed from Fig.(27) shows that the size of the trapped bolus gradually decreases, when the phase difference (ϕ) increases. Figs.(28), (29) are illustrated the impact of Reynolds model viscosity (α) and the velocity-slip parameter (β_1) which shows that whenever (α) and (β_1) increases, the size of the bolus decreases.

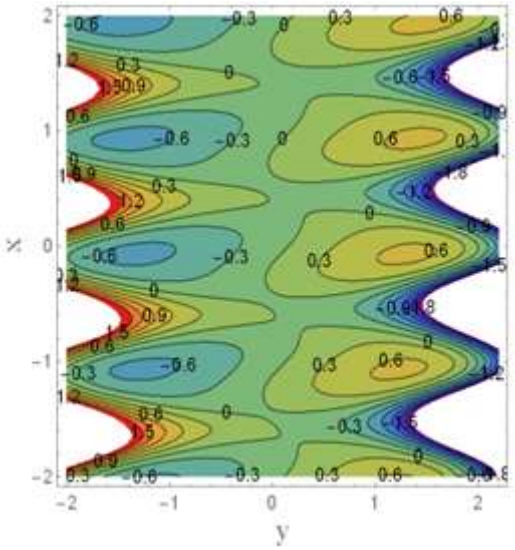

(a)

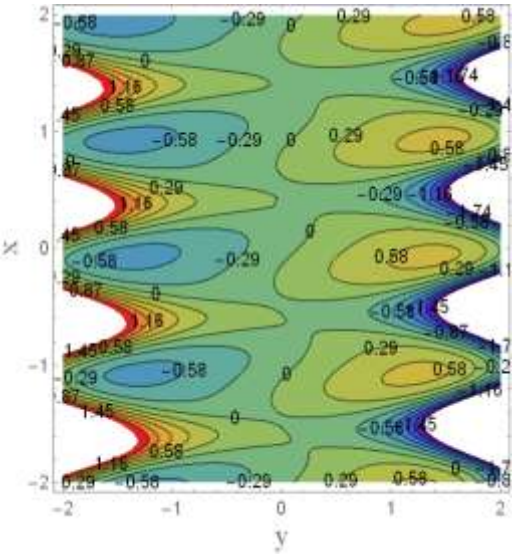

(b)

Figure 23: Streamlines for$\Phi = \pi/4$, $a = 0.4, b = 0.5, \alpha = 0.05, Q = 0.5, \beta = 1, \beta_1 = 0.5, Gr = 2, d = 1, N_r = 1, m = 0.1, k = 0.2, t = 0.3$andfor different M:**(a)**$M = 1$, **(b)**$M = 1.5$.

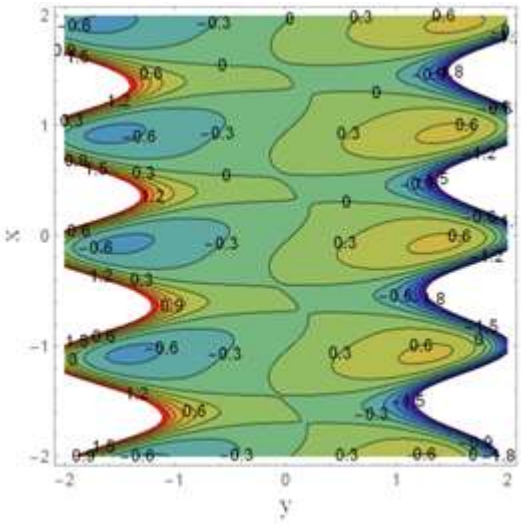

(a)

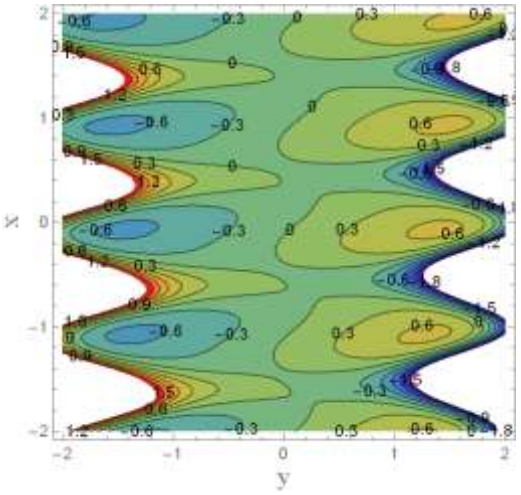

(b)

Figure 24: Streamlines for $\Phi = \pi/4, a = 0.4, b = 0.5, \alpha = 0.05, Q = 0.5, \beta = 1, \beta_1 = 0.5, d = 1, N_r = 1, m = 0.1, M = 4, k = 0.2, t = 0.3$ and for different Gr:**(a)**$Gr = 1$, **(b)**$Gr = 4$.

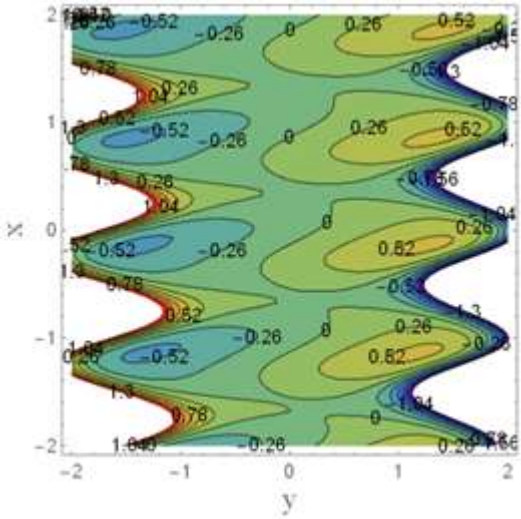

(a)

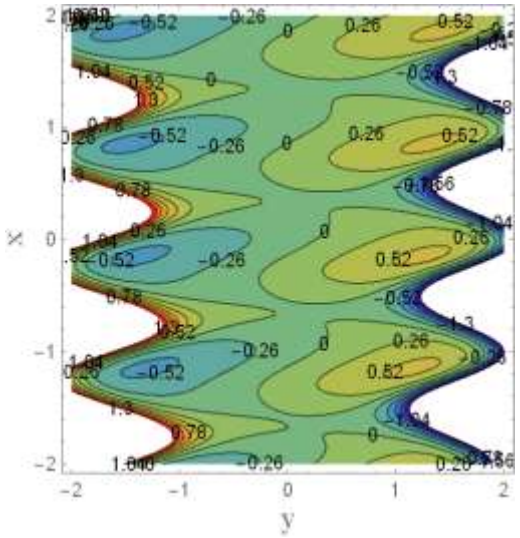

(b)

Figure 25: Streamlines for$\Phi = \pi/2\,, a = 0.4, b = 0.5, \alpha = 0.05, Q = 0.5, \beta = 1, \beta_1 = 0.5, Gr = 2, d = 1, m = 0.1, M = 4, k = 0.2, t = 0.3$and for different Nr:**(a)**$Nr = 1$, **(b)**$Nr = 3$.

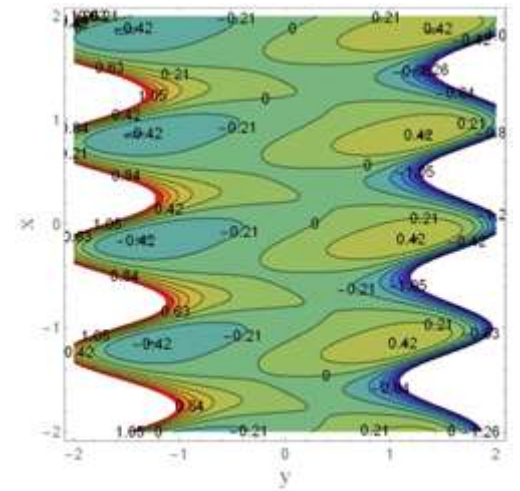

(a)

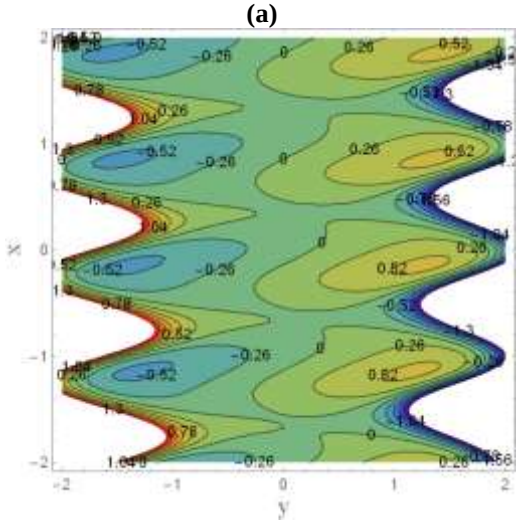

(b)

Figure 26: Streamlines for$\Phi = \pi/2\,, a = 0.4, b = 0.5, \alpha = 0.05, \beta = 1, \beta_1 = 0.5, Gr = 2, d = 1, N_r = 1, m = 0.1, M = 4, k = 0.2, t = 0.3$and for different$Q$:***(a)*** $Q = 0.2$, ***(b)*** $Q = 0.5$.

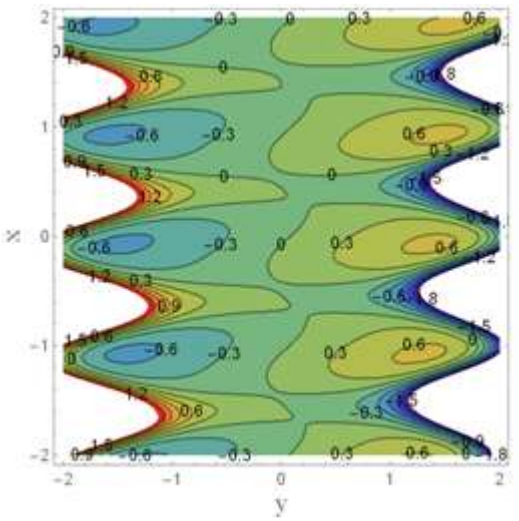

(a)

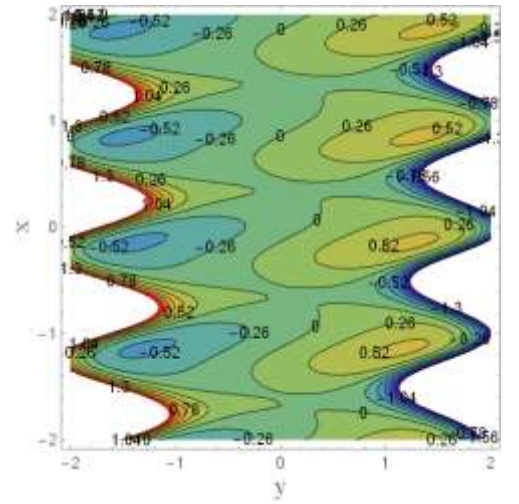

(b)

Figure 27: Streamlines for$a = 0.4, b = 0.5, \alpha = 0.05, Q = 0.5, \beta = 1, \beta_1 = 0.5, Gr = 2, d = 1, N_r = 1, m = 0.1, M = 4, k = 0.2, t = 0.3$ and for different Φ:***(a)*** $\Phi = \pi/4$, ***(b)*** $\Phi = \pi/2$.

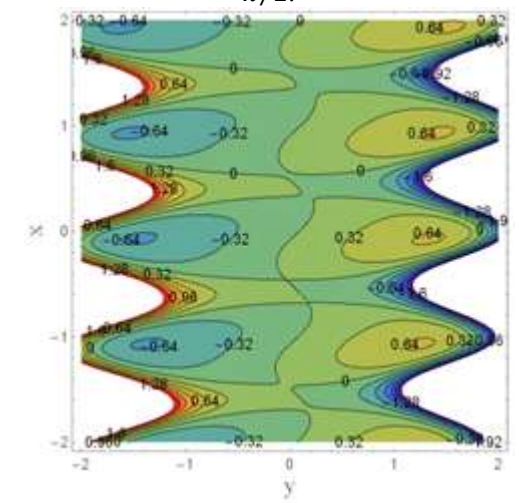

(a)

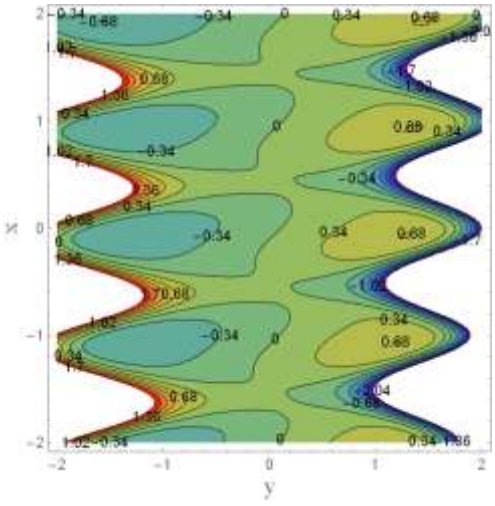

(b)

Figure 28: Streamlines for$\Phi = \pi/4\,, a = 0.4, b = 0.5, Q = 0.5, \beta = 1, \beta_1 = 0.5, Gr = 2, d = 1, N_r = 1, m = 0.1, M = 4, k = 0.2, t = 0.3$and for different$\Phi$:***(a)*** $\alpha = 0.2$, ***(b)*** $\alpha = 0.5$.

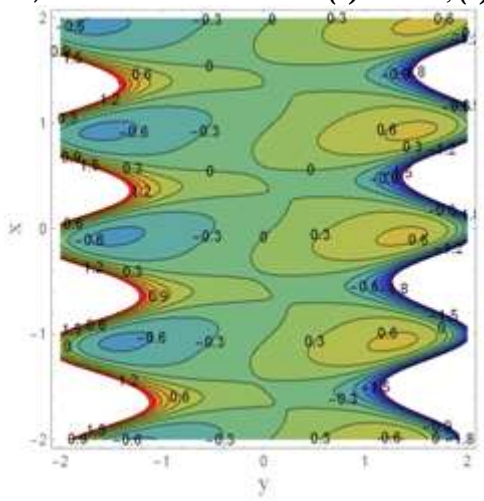

(a)

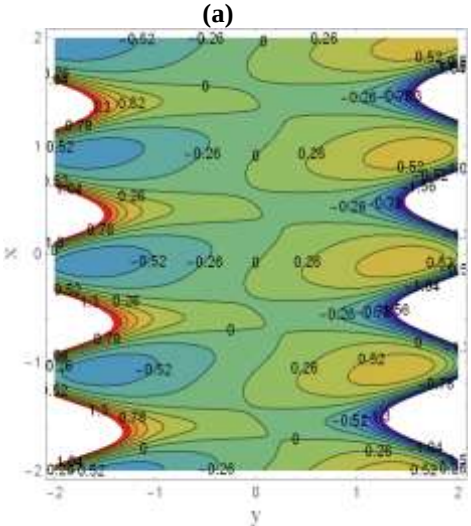

(b)

Figure 29: Streamlines for$\Phi = \pi/4\,, a = 0.4, b = 0.5, \alpha = 0.05, Q = 0.5, \beta = 1, Gr = 2, d = 1, N_r = 1, m = 0.1, M = 4, k = 0.2, t = 0.3$and for different β_1: ***(a)*** $\beta_1 = 0.5$***(b)*** $\beta_1 = 1.5$.

11. Conclusions

In this chapter we study a mathematical model of the peristaltic transport and analyzed in the tapered asymmetric channel with the influence of velocity-slip on (MHD) peristaltic flow through a porous medium with heat transfer is investigated and the influence of fluid temperature on viscosity. Analytical solutions for the effects of Hartmann number (M), the Grashof number (Gr), the thermal radiation parameter (Nr), the mean flow rate (Q), Reynolds model viscosity (α), the phase difference (ϕ), the heat source/sink parameter (β) and the velocity-slip parameter (β_1) have been for find the stream function. From the study, we can draw the following conclusions:

- The Pressure gradient distribution is decrease by increasing of (M), (Nr) and (Q). While opposite is increasing with an increase in (β_1).
- It has been found that the average rise in pressure Δp increases with the increase of (Gr) and (β) while it decreases by increasing (Nr) and (M).
- The profiles of axial velocity u take parabolic shape for it is curves.
- The velocity profile is gradually decreases with gradually increases of (Gr) and (α) up to a certain point Then the opposite happens in the direction.
- the velocity distribution increasing with increase of (M), (Nr) at the core part of the channel, While the opposite occurs with the increase in (Q) the velocity is decreasing.
- The temperature distribution during the peristaltic motion of the fluid where the temperature increases with increase of (β) and (m), While the opposite occurs with the increase in (Nr) and (ϕ) the temperature (θ) is decreasing.
- The shear stress is decrease of lower wall with increasing of (M), but the opposite increasing with increase (β_1).And reverse the two cases for a shear stress of upper wall.
- The trapping bolus increases with increases of (Q) and (α), while it has decrease with increases of (M), (ϕ) and (β_1).
- The difference in the values of (Gr) and (Nr) are both it had a very light effect that barely showed up on a stream function.

References

[1] Afifi NAS, Interaction of pulsatile and peristaltic transport of a magneto fluid with suspended particles, Sci Echoes 10 :9–16, 2006.
[2] A. Gul, I. Khan, S. Shafie, A. Khalid, A. Khan, Heat transfer in MHD mixed convection flow of a Ferrofluid along a vertical channel, PLoS ONE 10 (11) (2015) e0141213, http://dx.doi.org/10.1371/journal.pone.0141213.
[3] A. Gul, I. Khan, S. Shafie, Energy transfer in mixed convection MHD flow of nanofluid containing different shapes of nanoparticles in a channel filled with saturated porous medium, Nanoscale Res. Lett. 10 (2015) 490.

[4] A.H. Shapiro, M.Y. Jaffrin, S.L. Weinberg, Peristaltic pumping with long wavelengths at low Reynolds number, J. Fluid Mech.37 (1969) 799–825.
[5] A. Khalid, I. Khan, S. Shafie, Heat transfer in ferro-fluid with cylindrical shape nanoparticles past a vertical plate with ramped wall temperature embedded in a porous medium, J. Mol. Liq. 221 (2016) 1175–1183.
[6] A. Sinha, G.C. Shit, N.K. Ranjit, Peristaltic transport of MHD flow and heat transfer in an asymmetric channel: effects of variable viscosity, velocity-slip and temperature jump, Alexandria Eng.J. 54 (2015) 691–704.
[7] A. Sinha, J.C. Misra, Effect of induced magnetic field on MHD stagnation point flow and heat transfer on a stretching sheet, ASME J. Heat Transfer 136 (2014) 112701.
[8] Atul Kumar Singh, Ajoy Kumar Singh, N.P. Singh, Heat and mass transfer in MHD flow of a viscous fluid past a vertical plate under oscillatory suction velocity, Indian J. Pure Appl. Math. 34 (3) (2003) 429–442.
[9] D. Tripathy, O.A. Beg, A study on peristaltic flow of nano-fluids: application in drug delivery system, Int. J. Heat Mass Transfer 70 (2014) 61–70.
[10] Eytan O, Jaffa AJ, Elad D, Peristaltic flow in a tapered channel: Application to embryo transport within the uterine cavity, Med Eng Phys 23:473–482, 2001.
[11] J.C. Misra, B. Mallick, A. Sinha**,** Heat and mass transfer in asymmetric channels during peristaltic transport of an MHD fluid having temperature-dependent properties, AEJ.J. Centre for Healthcare Science, (2016) 711103, India.
[12] J.C. Misra, S.D. Adhikary, MHD oscillatory channel flow, heat and mass transfer in physiological fluid in presence of chemical reaction, Alexandria Eng. J.55 (2016) 287–297.
[13] [13] J.C. Misra, S.K. Pandey, Peristaltic transport of physiological fluids, in: J.C. Misra (Ed.), Biomathematics: Modelling and Simulation, World Scientific, London, USA, Singapore, 2006, pp. 167–193 (Chapter 7).
[14] J.C. Misra, S. Maiti, G.C. Shit, Peristaltic transport of a physiological fluid in an asymmetric porous channel in the presence of an external magnetic field, J. Mech. Med. Biol. 08 (2008) 507–525.
[15] J.C. Misra, S. Maiti, Peristaltic pumping of blood through small vessels of varying cross- section, ASME J. Appl. Mech. 79 (6) (2012) 1–19.
[16] J.C. Misra, S. Maiti, Peristaltic transport of a rheological fluid: model for movement of food bolus through esophagus, Appl. Math. Mech. (AMM) 33 (3) (2012) 315–332.
[17] J.C. Misra, S.K. Pandey, Peristaltic flow of a multilayered power-law fluid through a cylindrical tube, Int. J. Eng. Sci. 39(4) (2001) 387–402.
[18] J.C. Misra, S.K. Pandey, Peristaltic transport of blood in small vessels: study of a mathematical model, Comput. Math. Appl. 43 (8-9) (2002) 1183–1193.
[19] Mekheimer KhS, Peristaltic flow of blood under effect of a magnetic field in a non-uniform channels, Appl Math Comput153:763–777, 2004.
[20] N.A.M. Zin, I. Khan, S. Shafie, The impact silver nanoparticles on MHD free convection flow of Jeffrey fluid over an oscillating vertical plate embedded in a porous medium, J. Mol. Liq. 222 (2016) 138–150.
[21] N. Ali, T. Hayat, S. Asghar, Peristaltic flow of a Maxwell fluid in a channel with compliant walls, Chaos Solitons Fract. 39 (1) (2009) 407–416.
[22] R. Pfeffer, J. Happel, An analytical study of heat and mass transfer in nultiparticle systems at low Reynolds number, Am. Inst. Chem. Eng. J. 10 (1964) 605–611.
[23] S. Maiti, J.C. Misra, Non-Newtonian characteristics of peristaltic flow of blood in micro-vessels, Commun. Nonlinear Sci. Numer. Simul.18(8) (2013)1970–1988.
[24] S. Maiti, J.C. Misra, Peristaltic flow of a fluid in a porous channel: a study having relevance to flow of bile within ducts in a pathological state, Int. J. Eng. Sci. 49 (9) (2011) 950–966.
[25] S. Maiti, J.C. Misra, Peristaltic transport of a couple stress fluid: some applications to hemodynamics, J. Mech. Med. Biol. 12 (3)(2012) 1–21.
[26] S.R. Mishra, G.C. Dash, M. Acharya, Mass and heat transfer effect on MHD flow of a viscoleastic fluid through a porous medium with oscillatory suction and heat source, Int. J. Heat Mass Transfer 57 (2013) 433–438.
[27] S. Srinivas, R. Gayathri, Peristaltic transport of a Newtonian fluid in a vertical asymmetric channel with heat transfer and porous medium, Appl. Math. Comput. 215 (2009) 185–196.
[28] T. Hayat, R. Iqbal, A. Tanveer, A. Alsaedi, Influence convective conditions in radiative peristaltic flow of pseudoplastic nanofluid in a tapered asymmetric channel, J. Magn. Magn. Mater. 408 (2016) 168–176.
[29] T. Hayat, S. Hina, N. Ali, Simultaneous effects of slip and heat transfer on the peristaltic flow, Commun Nonlinear Sci Numer Simulat 15 (2010) 1526–1537.
[30] Usha S, Rao AR, Effects of curvature and inertia on the peristaltic transport in a two-fluid system, Int J Eng Sci 38:1355–1375, 2000.
[31] Y.C. Fung, C.S. Yih, Peristaltic transport, ASME J. Appl. Mech. 35(4) (1968

Author Profile

Ahmad M. Abdulhadi I received the B.S and MS.c degree from Baghdad University College of science-dept. of mathematics 1988. The Ph.D from Pune University-India in 2000.I have degree of professor in mathematics since 2012.Now, working in college of science-department of Mathematics.

Mohammed R Salman: I received the B.S degree from Al- Mustansiriyah university-college of science-dept. of mathematics 1989 and MS. degree from Al-Kufa university-college of education for women-dept. of Mathematics 2014.